

4

The basic phase diagrams

The reader is assumed to be familiar with the interpretation of binary phase diagrams and the chapter begins with a brief description of the specific features involved in the graphical representation of ternary and even higher order systems. Six ternary systems are analysed in detail by way of example : Fe-Cr-C, Fe-Ni-Cr, Fe-Mn-S, Fe-Co-Cu, Fe-Mo-Cr and Fe-C-V. They have been chosen because they include all the typical phase reaction configurations encountered in iron-base alloys, and especially in steels.

Calculated phase diagrams³ are extensively employed in this section, since they enable large numbers of isothermal sections and isopleths to be plotted, facilitating the detailed study of their variation with temperature or composition.

4-1 Equilibria between condensed phases

Basic rules

Our knowledge of the metallurgy of steels, particularly as regards the effects of composition and temperature on microstructure, is largely based on experimental data obtained using a wide range of physical and chemical techniques. The thermodynamics of phase equilibria provides the only unifying framework that enables these data to be compared and validated.

When considering a particular system, a given quantity of matter is treated, that is a fixed total number of molecules (usually gram molecules or moles). The nature of the molecules is determined by the composition, *i.e.* by the concentrations of the different constituents, either elements or compounds. If a system comprises N constituents, the composition will be fully defined when N-1 concentrations are fixed. The concentrations may be given in terms of atom or mole fractions or atomic or weight percentages. In practice, metallurgical phase diagrams are usually represented in terms of weight percentages. This approach will be applied in most of the diagrams considered, atomic

3. The majority of the calculations were performed using the Thermocalc or Pandat softwares, with data available in the SGTE bank in 2002.

percentages being used only when it is necessary to emphasize stoichiometric proportions.

The equilibrium conditions to which the system is subjected are described based on the first and second laws of chemical thermodynamics. In particular, at equilibrium, the *chemical potential* of each constituent is identical in each of the phases present. *The equilibrium state is unique*, that is, the number of phases, their proportions and their compositions are fixed.

The phase rule was formulated by J.W. Gibbs in 1876. It stipulates the number of degrees of freedom F , or variance, in a system at equilibrium, *i.e.* the number of parameters that can vary independently, the variables in question being the temperature, the pressure and the concentrations of each of the constituents. For an alloy :

$$P + F = C + 2 \quad (4-1-1)$$

where P is the number of phases, C is the number of components and 2 represents the two variables pressure and temperature. In condensed metallic systems, pressure generally has very little influence in the range of temperatures normally considered and is usually neglected, in which case the relation becomes $P + F = C + 1$.

The phase transformations considered conserve the number of atoms of each species, and involve only their redistribution among the different phases. This forms the basis for the so-called “lever rule” in binary equilibria (*cf.* § 5-1), which is a particular form of the barycentre rule for multicomponent systems.

Representations of phase equilibria

The graphical representations of phase equilibria are governed by the phase rule mentioned above. Thus, in a binary system (two constituents), an equilibrium between two phases will have only a single degree of freedom. If the temperature is fixed, the compositions and proportions of the two phases are automatically also defined. For example, in a temperature/composition diagram, the equilibrium between the solid and liquid phases is described by two points at the same temperature. The line joining the two points is known as a *tie-line*. When the temperature varies, the points representing the corresponding solid and liquid compositions describe curves called the *solidus* and *liquidus* respectively. For a given alloy composition, the liquidus temperature T_L is the temperature at which the first solid forms on cooling from the liquid field, while T_S is that at which the last liquid disappears. T_S will subsequently be called T_{Sth} , since it is the theoretical solidus temperature when equilibrium is maintained throughout solidification, a condition rarely fulfilled in practice (*cf.* § 4-6). In a binary system, an equilibrium between three phases is represented by three points and has zero degrees of freedom. It can occur only at one temperature and the compositions and proportions of the three phases are fixed.

Since it is assumed that readers are familiar with the interpretation of binary phase diagrams, the remainder of the discussion will concern the particular features of ternary and even higher order systems. Exhaustive treatments can be found in basic text books

on phase diagrams [Pri66], [Wes82], while short introductions are also given in certain collections of phase diagrams [ASM92].

Consideration of multicomponent systems is essential in order to understand the microstructures of steels, which generally contain a large number of alloying elements. For a system containing N constituents, graphical representations are limited to two or at most three spatial dimensions, so that for high values of N they are restricted to particular projections or sections to reduce the number of variables appropriately. However, in practice, this limitation is not as restrictive as it might appear. The essential requirement is to be able to represent all the phases liable to occur, particularly the intermetallic compounds. Although many of these do not exist in binary systems, they can generally be found in at least one of the constituent ternary systems. It is for this reason that the present chapter emphasises the importance of ternary systems, which provide an extremely useful guide and are often quite sufficient to understand the microstructures of commercial steels. An attractive feature of ternary systems is that they can be represented graphically in several different ways.

The addition of an extra element to a system increases the number of degrees of freedom by one. For example, in a ternary, equilibrium between three phases is represented by a set of three lines that vary with temperature, instead of three points at a single temperature in a binary system. The lines are said to be *monovariant*. In a quaternary system, the lines become surfaces. Similarly, the liquidus line in a binary diagram becomes a liquidus surface in a ternary. In the latter case, it is divided into a number of distinct regions representing equilibrium between the liquid and each of the *primary* solid phase fields.

The barycentre rule

A ternary system can conveniently be represented using triangular coordinates. An isothermal section can then be plotted in two dimensions, the complete section being a triangle with the three pure constituents at the corners (*cf.* Fig. 4-1-4). In two-phase fields, the compositions in equilibrium are connected by tie-lines, which can never intersect one another (otherwise the composition at the crossover point would have two possible equilibria, in contradiction with the phase rule). The proportion of the two phases for any composition can be calculated by applying the inverse segment (lever) rule to the corresponding tie-line. For example, in Figure 4-1-4, an alloy of overall composition p will consist of two phases of compositions h and k, whose percentages (*h*) and (*k*) are given by :

$$(h) = kp/kh \text{ and } (k) = ph/kh \quad (4-1-2)$$

In the three-phase field, the compositions of the phases are fixed (a, b and c) and their proportions in an alloy of overall composition m are determined by applying the lever rule to the points of intersection of the lines drawn from a, b and c through m to the opposite tie-line. For example, referring to Figure 4-1-4:

$$(a)=rm/ar; (b)=sm-bs; (c)=tm/ct \quad (4-1-3)$$

(Note that the proportions are also given by ((a)=cs/ac; (a)=bt/ab etc)).

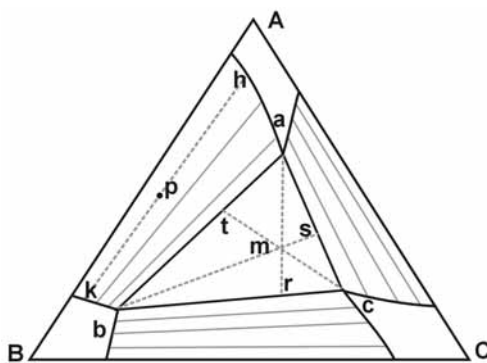


Figure 4-1-4:

Representation of the barycentre rule on a ternary diagram. Three types of phase field can be distinguished :

those corresponding to the single phase regions A, B and C,

the intervening two-phase fields where a number of tie-lines are shown,

and the three-phase field enclosed by the tie-line triangle abc.

The proportions of the different phases at any point are given by the relations 4-1-2 and 4-1-3.

When two equilibrium curves intersect (a, b and c for example) their metastable extensions in the neighbourhood of the points of intersections lie inside, either outside of the corresponding three-phase triangle.

The proportions defined in this way are in the units used to construct the phase diagram, usually atomic or weight percent or mole fractions. Values determined by micrographic measurements or image analysis are volume fractions, so that density corrections must be made to establish the equivalence.

A number of geometrical rules govern the possible nature of the junctions between adjacent phase fields (number of phases, angles of junction and tangents), [Pri66]. Thus, a single phase field cannot be adjacent to a three-phase field and can only join it at a point (in an isothermal section), and similarly cannot be adjacent to another single phase field. An exception to this rule is the case of second order reactions such as disorder-order transformations. A single phase field is thus always bounded on the sides by two-phase fields and by three-phase fields at the apexes. However, single phase fields may sometimes appear as a line when they are very narrow. These rules are the natural consequences of the properties of the thermodynamic functions governing phase equilibria, especially with regard to their continuity as a function of temperature.

Phase reactions

Since each state of equilibrium is unique, the change from one equilibrium at temperature T_1 to another at temperature T_2 is considered to be reversible. The state attained at T_2 is the result of a reaction that occurs *on cooling* from T_1 to T_2 . In a binary system, three-phase equilibria are invariant, *i.e.* they occur at only one temperature. Cooling or heating from this temperature therefore requires that one or more of the phases must disappear. For example, if the liquid in equilibrium with two solid phases a and b disappears on cooling, the reaction will be written $L \rightarrow a + b$ and is said to be eutectic in nature. Indeed, a name has been given to all the reactions that occur during cooling from an invariant three-phase equilibrium, depending on the products formed. These names have the suffix “ic” for the reactions between a liquid and two solids and the suffix “oid” for those involving three solid phases. Thus, if L , L_1 and L_2 are liquids and a , b and c are solids :

- $L \rightarrow a + b$, eutectic reaction
- $c \rightarrow a + b$, eutectoid reaction
- $L + a \rightarrow b$, peritectic reaction
- $a + b \rightarrow c$, peritectoid reaction
- $a \rightarrow b + L$, metatectic reaction
- $L_1 \rightarrow a + L_2$, monotectic reaction
- $L_1 + L_2 \rightarrow a$, syntectic reaction

By extension, the same reaction names are used in ternary systems when the initial equilibrium is not invariant but monovariant. Ternary reactions can also occur starting from invariant four-phase equilibria. Those that will be most frequently encountered in the present book are the following :

- $L \rightarrow a + b + c$, ternary eutectic reaction
- $L + a + b \rightarrow c$, ternary peritectic reaction
- $L + a \rightarrow b + c$, pseudo-peritectic reaction sometimes termed quasi-peritectic

The expression “three-phase eutectic” will be used for multicomponent systems when a non-invariant equilibrium involves three solid phases and the liquid. The liquid phase is often forgotten, since it is absent in room temperature microstructures.

Hillert's criterion

The feature that determines the *type of reaction* is the variation in the proportions of the different phases. Consider a reaction between two solid phases a and b and a liquid phase L , present at a temperature T in respective proportions m_a , m_b and m_L and with concentrations in element i , X^a_i , X^b_i , X^L_i . A small temperature drop ΔT causes changes Δm_a , Δm_b and Δm_L respectively in these proportions (Relation 4-1-5). The alloy contains three elements, two of whose concentrations are independent. For the element i , the principle of conservation leads to Relation 4-1-6, known as Hillert's criterion [Pri66], [Hil79].

$$\Delta m_a + \Delta m_b + \Delta m_l = 0 \quad (4-1-5)$$

$$m_a \Delta X^a_i + X^a_i \Delta m_a + m_b \Delta X^b_i + X^b_i \Delta m_b + m_l \Delta X^L_i + X^L_i \Delta m_l = 0 \quad (4-1-6)$$

According to Relation 4-1-5, the Δm values for a , b and L cannot all be positive. We will therefore assume that Δm_L is negative, *i.e.* that the proportion of liquid decreases. The reaction is eutectic if both Δm_a and Δm_b are positive, and peritectic if either Δm_a or Δm_b is negative. The reaction is thus considered to be of peritectic nature when the proportion of one of the two solid phases decreases and the other increases as the temperature falls.

Starting from a three-phase equilibrium *at a given temperature*, the nature of the reaction depends on the relative proportions of the phases present, that is on the position of the alloy composition in the tie-line triangle. According to relation 4-1-6, the reaction may be eutectic in certain zones and peritectic in others.

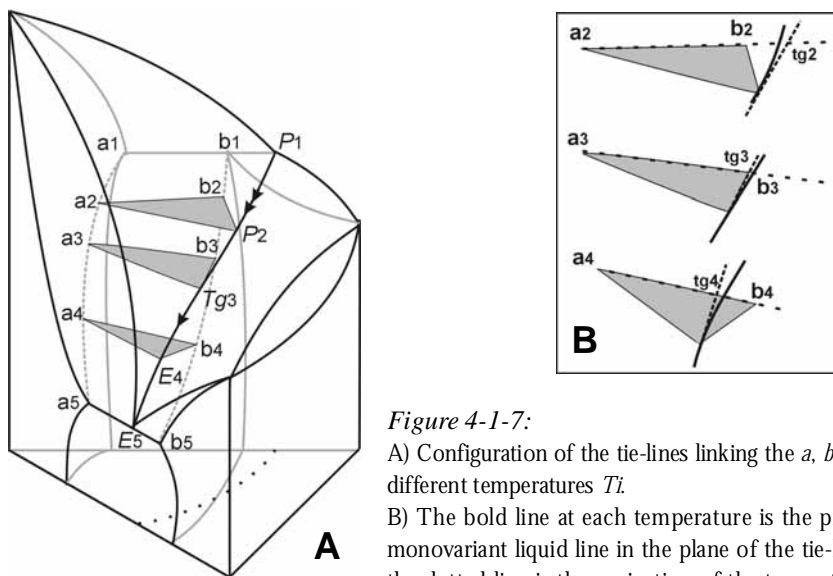


Figure 4-1-7:

A) Configuration of the tie-lines linking the *a*, *b* and *L* phases at different temperatures T_i .

B) The bold line at each temperature is the projection of the monovariant liquid line in the plane of the tie-line triangle and the dotted line is the projection of the tangent t_g to the liquid line in this plane. At temperature T_2 , t_g cuts the solid tie-line outside the segment a_2b_2 , indicating a peritectic reaction

$a_2 + L \rightarrow b_2$ whereas at temperature T_4 , the intersection lies within the segment a_4b_4 , indicating a eutectic reaction $L \rightarrow a_4 + b_4$. T_3 lies at the transition between the two types of reaction.

The tangent rule for a ternary system

The distinction between peritectic and eutectic reactions is simplified in the particular case where no solid has yet been formed and where the overall composition of the liquid lies on the monovariant line at temperature T . This is illustrated by the ternary system shown in Figure 4-1-7, which comprises a binary peritectic at temperature T_1 on one side and a binary eutectic at temperature T_5 on the opposite side. Three different tie-line triangles are shown for temperatures T_2 , T_3 and T_4 . On the right hand side of the diagram, the projection of the monovariant line and its tangent are shown on these isothermal sections. The nature of the reaction is determined by the relative movements of the liquid, *a* and *b* compositions as the temperature falls. A useful guide is the so-called tangent rule which states that :

- when the projection of the tangent to the monovariant line lies outside the tie-line triangle (*i.e.* it intersects *ab* beyond *b*), then the reaction is peritectic, as at T_2 .
- when it lies inside the triangle (*i.e.* it intersects *ab* between *a* and *b*), then the reaction is eutectic, as at T_4 . T_3 is an intermediate case and represents the temperature where the tangent intersects *ab* at *b*.

The monovariant lines where the reaction is peritectic in nature are conventionally indicated by a double arrow, and those where it is of eutectic type by a single arrow.

The fact that the lines corresponding to the variation of the liquid and *b* compositions with temperature cross in a low temperature plane of projection is an indication that the

configuration of the tie-line triangles has changed with respect to the monovariant line (Fig. 4-1-7). Similarly, configurations exist in which the projections of the solid solution lines *a* and *b* cross one-another. In this case there is a transition between a peritectic and a metatectic reaction.

4-2 Theoretically calculated phase diagrams

Basic principles

In a system at equilibrium, there is no excess free energy and consequently no driving force to induce a change. The equilibrium state is that with minimum free energy, and for a given pressure and temperature, in a system involving several constituents and several possible phases, it is necessary to consider the free energy of each constituent in each phase. The formulation of the free energy of each phase as a function of composition, together with the imposed overall composition, enables calculation of the compositions and proportions of the individual phases corresponding to a *minimum total free energy*. The concept of *chemical potential* or *activity* is a consequence of this relationship, since by definition, the chemical potential of each constituent is identical in each of the phases in equilibrium. The problem has a simple geometrical solution in the case of a binary system, where the compositions and proportions of the phases at equilibrium at a given temperature are defined by the common tangents to the free energy-composition curves for the different possible phases and the overall compositions considered. In a ternary system, the equilibrium is defined by tangent planes common to free energy-composition surfaces.

The calculation of equilibrium diagrams thus requires a knowledge of the free energy-composition relations as a function of temperature for all the phases liable to exist in the system considered. In fact, the intrinsic free energies are not known and it is the differences in free energy with respect to a known common reference state that are employed. These differences are estimated or determined experimentally.

The enthalpy of mixing ΔH involved in the formation of a compound or solution AB is the difference in enthalpy between the two pure components and that of the compound. A useful common practice is to refer to an *ideal* mixture in which the chemical potential of the constituent considered is given by a function $RT\ln(x_j)$, where R is the perfect gas constant, T is the absolute temperature and x_j is the concentration of element *j*.

The deviation from ideality is expressed by an excess free energy of mixing ΔG^{xs} :

$$\Delta G^{xs} = \Delta H - T\Delta S^{xs} \quad (4-2-1)$$

where ΔG^{xs} is the change in excess entropy.

The sign of the excess free energy of mixing ΔG^{xs} gives an indication concerning the type of bonding between the elements A and B. A positive value indicates repulsive forces, while a negative sign signifies attraction. The excess free energy is often employed to qualify the behaviour of different systems. Thus, a large negative value

implies a tendency to form intermetallic compounds, as in the Fe-Mo-Cr system (§ 4-13), while a positive value indicates a tendency for decomposition, as in the Fe-Co-Cu system (§ 4-12). It is because of these characteristics that these two systems were chosen among the examples considered in the present book. Various methods exist for expressing the free energy and the interactions between atoms, including techniques based on first principles and ones involving the optimisation of thermodynamic parameters.

“Ab initio” methods

The *ab initio* methods for calculating phase diagrams are based on a quantum mechanics and statistical analysis approach. The total energies for the formation of perfectly ordered structures at $T=0K$ are obtained from local approximation electron density functions. Statistical calculations using the cluster variation method (CVM) or Monte Carlo simulations enable the thermodynamic parameters to be determined at finite temperatures [Col02]. Such first principle calculations are generally extremely demanding in terms of computer time and cannot be employed for systems containing more than two or three elements at most. Nevertheless, their use has extended rapidly since 1990. The only input data required are the atomic numbers of the elements considered and the crystal structures of all the phases involved. The data obtained can then be used for other phase diagram computation techniques employing an optimisation approach [Col01].

Methods involving the optimisation of thermodynamic parameters

In these methods, the variation of ΔG (or ΔGx_s) as a function of temperature and composition must be expressed for each phase with a minimum number of phenomenological parameters. A simplified description of the thermodynamic model employed is given in the review article [Kat97].

Sets of parameters for the phases of different systems are optimised to obtain the best fit with observed equilibria and the optimised values are collected in data banks such as SGTE [SGTE]. A general library is accessible to users of different calculation softwares. Specific data bases also exist for particular types of alloys (steels, superalloys, aluminium alloys, etc) and are marketed independently. New results are continually collected and critically analysed before making them available for future calculations [Ans97], [Sau98].

Numerous calculation codes are now available and are becoming increasingly sophisticated to more precisely describe phase interactions. Noteworthy examples, in alphabetical order, are ChemCAD®, FactSage®, MTDATA®, Pandat®, Thermocalc®, and ThermoData®⁴. They can be used for binary, ternary and multicomponent systems. However, the number of parameters increases faster than the number of combinations of the elements two by two. Calculation rapidly becomes extremely difficult, even for powerful computers.

In particular, the following five points must be checked :

Experimental data contained in the data bank

Modern calculation softwares give the references that have been used to establish the data base concerned. It is strongly recommended to consult them to check which experimental data have been used in the parameter optimisations. Calculated optimisations generally *depend entirely on existing experimental data*. Thus, if the data bank contains no data on a compound that was unknown when the base was compiled, the calculation will be unable to consider its existence. Some calculated diagrams have not been verified and updated using modern techniques, while certain experimental results can be more than sixty years old. Many old results, published several decades ago, are still used as basic data. Even though the experimental facts may remain valid, their interpretation must be critically analysed in the light of the accuracy of the measurement techniques used at the time.

Date of revision

There may be a considerable delay between the publication of new experimental results and their inclusion in the data bank. The correction and updating of a data bank is a lengthy procedure and can take several years, since *it is not possible to modify only the data for a single phase in isolation*. Some of the basic systems have been revised many times.

Phase models

Some phases are difficult to model. For example, many different attempts have been made to model the σ phase in steels [Ans97], [Wat01]. The unit cell of the σ crystal structure contains 30 atoms distributed on five independent sub-lattices. Ideally, the model should also consider five sub-lattices, but would then probably comprise a large number of adjustable parameters depending on the approach employed. Consequently, σ phase is described with only three sub-lattices, using models of the types $(A,B)_{18}(A)_{14}(B)_8$ or $(A,B)_{10}(A)_4(B)_{16}$, where iron is represented by the B atoms. Energy of mixing parameters (excess Gibbs free energy) are used to adjust the possibilities of substitution of A and B atoms. However, the same parameters can also be involved in other equilibria (*e.g.* α/γ) and in other systems. In order to take into account all the systems concerned, their adjustment is extremely laborious.

Simplifications

Steels can contain a large number of alloying elements. The rigorous calculation of phase equilibria then becomes so complex that it is impossible to allow for all the potential interactions between the different types of atoms. The simplification required to calculate phase diagrams in this case usually involves neglecting certain parameters.

4. web sites :

ChemCAD <http://www.chemcad.fr>
 FactSage <http://www.Factsage.com>;
 MTDATA <http://www.npl.co.uk>;
 Pandat <http://www.computherm.com>;
 Thermocalc <http://www.thermocalc.se>;
 ThermoData <http://online.fr>.

Scope of use

Even when the majority of the equilibria involved have been optimised, calculated phase diagrams can give erroneous results for equilibria other than those considered. Data extracted from banks intended for purposes other than the determination of phase diagrams may prove unusable, due to the experimental values having been obtained outside the ranges of temperature and composition of interest. A good example is the extrapolation to lower temperatures of solid state phase transformation data.

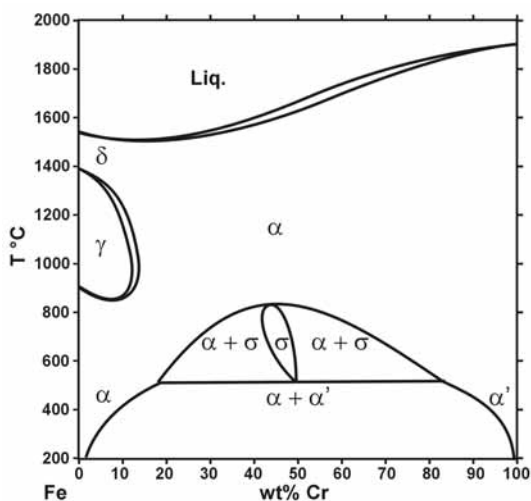
4-3 Experimentally determined phase diagram

The role of carbon associated with iron to make steels was understood only towards the middle of the 19th century. The first proposals for the Fe-C phase diagram date from 1895–1899 (quoted in [LeC99], see also [Wad02]). The determination of many other phase diagrams began in the first half of the 20th century. Then, as is still the case today, the experimental techniques employed were essentially optical micrography, X-ray diffraction, chemical analysis, dilatometry and thermal analysis. The amount of work involved in determining even a fairly simple diagram is enormous. Phase compositions were originally determined by extraction and wet chemical analysis. Consequently, inorganic chemistry played an extremely important part in these basic studies. Many of the very old experimental results remain perfectly valid today, due to the meticulous quality of the work performed.

Transmission electron microscopy subsequently provided a better understanding of precipitation reactions and age hardening phenomena, originally studied using X-ray diffraction techniques (*e.g.* Guinier-Preston zones in Al-Cu alloys). Great progress was made when electron microprobe analysis became available in the 1960s and the scanning electron microscope in the 1970s. The ability to investigate structures at the micron scale led to the discovery of many new phases, giving rise to a continuous process of correction and refinement of phase diagrams.

The literature on phase diagrams has become extremely voluminous, making periodic reviews and critical comparative examinations of data essential. A noteworthy example is Hansen's Handbook [Han58], which is one of the earliest collections of binary diagrams based on the compilation of experimental results. For the reasons outlined above, even the oldest compilations merit attention, since they contain references not included in modern computer-based libraries. Since the 1980s, updated handbooks and compilations of critically reviewed phase diagrams have been regularly published (by the ASM, the Indian Institute of Metals, *etc.*). Phase diagram collections of this type are specifically identified in the list of references.

Figure 4-4-2:
Calculated Fe-Cr phase diagram.



4-4 The Fe-Cr-C system : liquidus surface

The limiting binary systems : Fe-C, Fe-Cr and Cr-C

The Fe-C system has two variants, the *stable* version, where undissolved carbon is in the form of graphite, and the *metastable* version with the formation of cementite (Fe_3C). The diagram published in 1948 and quoted in [Han58] was for a long time considered as the reference. Since then, the major correction concerns the extension of the austenite field. For example, the carbon solubility limit in austenite at the eutectic temperature in the presence of Fe_3C is now recognized to be 2.14 % instead of 1.7⁵. The modern version of the diagram is illustrated in Figure 4-4-1 [Mas90].

The Fe-Cr system shows three important features (Fig. 4-4-2) :

- the existence of a two-phase region called the *gamma loop* separating the ferrite and austenite fields;
- the formation of the intermetallic σ phase below 812 °C;
- the separation of the ferrite field at low temperatures into the α and α' forms (decomposition reaction described in § 13-1).

Several versions of this diagram can be found in the literature. The most recent modifications concern the σ phase region and the α/α' decomposition.

The Cr-C system also has two stable and metastable variants, in which pure carbon is in the form of either diamond (Fig. 4-4-3) or graphite. This difference does not affect the region of interest for steels.

5. In practice, metallurgical phase diagrams are usually represented in terms of weight percentages

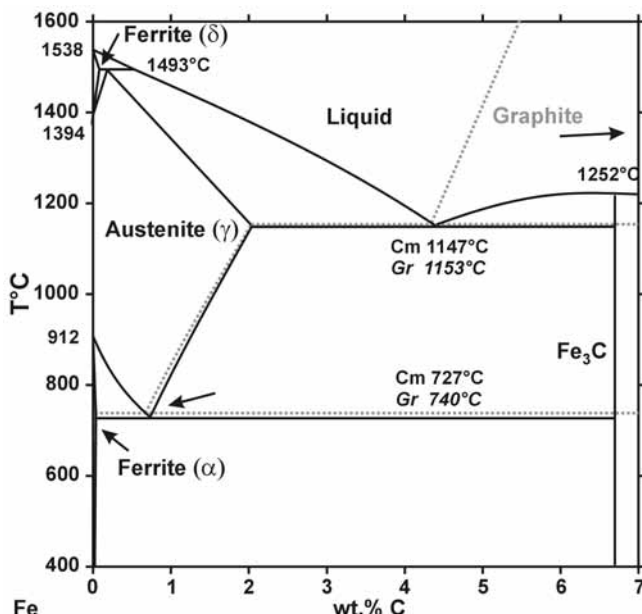


Figure 4-4-1:
Calculated Fe-graphite (grey) and Fe-cementite (black) systems.

Phase compositions for invariant reactions (in order of increasing carbon content)	Iron-cementite		Iron-graphite	
	wt %C and (at%)C	T°C	wt %C and (at%)C	T°C
Peritectic	0.09(0.4)-0.16(0.74)-0.53(2.43)	1493	0.09(0.4)-0.16(0.74)-0.53(2.43)	1493
Eutectic	2.14(9.23)-4.3(17.3)-6.69(25)	1147	2.1(9.06)-4.2(17.1)-100(100)	1153
Eutectoid	0.022(0.104)-0.76(3.46)-6.69(25)	727	0.02(0.096)-0.65(2.97)-100(100)	740

The Fe-Cr-C system

As in the Fe-C system, two possibilities must be considered, corresponding to stable and metastable variants. In fact, chromium has a strong affinity for carbon and stabilises all the carbides, including cementite. It is the metastable version of the diagram that is the reference for steels, since graphite is never observed in the range of compositions and processing conditions concerned in practice. The situation is different in the case of chromium-containing cast irons, where the composition and processing conditions can sometimes promote the appearance of graphite.

Several versions of the stable and metastable diagrams have been published, including [Bun58], [Gri62], [Jac70], [For73], [Riv84] (compilation), [Tho85], [And88]. The modifications mainly concern the extent of the Cr_{23}C_6 phase field, which has long been

Figure 4-4-3:
Calculated Cr-diamond phase diagram.

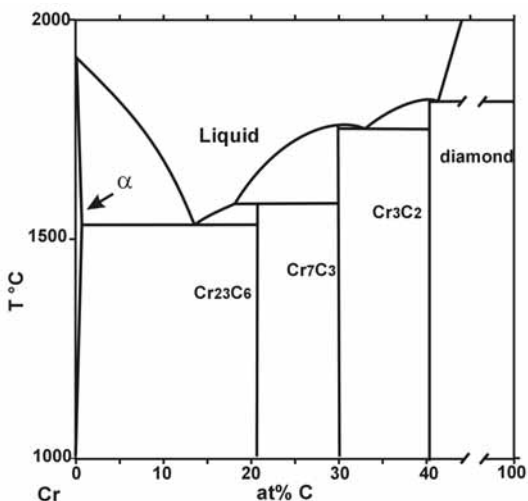
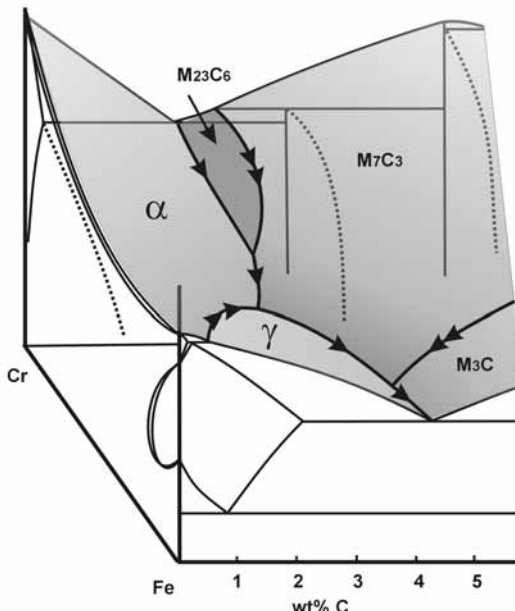


Figure 4-4-4:
Metastable Fe-Cr-C phase diagram for carbon contents less than 5%. Simplified perspective view adapted from [Jac70]. The bold black lines are the monovariant lines separating the primary solidification fields. Conventionally, eutectic type equilibria are indicated by a single arrow and those of peritectic type by a double arrow. The dotted lines represent the limiting solid compositions in equilibrium with the liquid on the corresponding monovariant line. There are three four-phase invariant equilibria:
Liquid + α + M₂₃C₆ + M₇C₃
Liquid + α + γ + M₇C₃
Liquid + γ + M₇C₃ + M₃C



a subject of debate. The field was originally joined to the primary austenite field at about 20 % Cr. The disagreement is probably due to the fact that the primary M₇C₃ carbides are unstable on cooling and readily transform to M₂₃C₆ at temperatures that are still quite high. Both experimental and calculated versions published since the late 1990s show relatively good agreement.

Liquidus surfaces in the Fe-Cr-C system

The different regions of the liquidus surface are illustrated schematically in Figure 4-4-4, where they are bounded by those of the Fe-C and metastable Cr-C systems. A

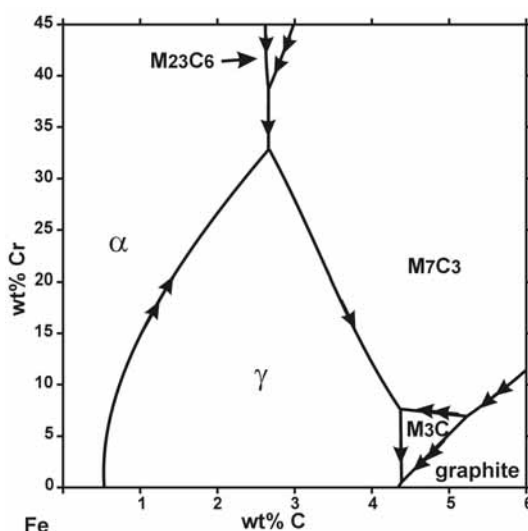


Figure 4-4-5:

Calculated liquidus projection in the iron-rich corner of the stable Fe-Cr-C system (with graphite). In the metastable diagram, the graphite field does not exist.

projection of the liquidus surface of the stable version is shown in Figure 4-4-5, while an equivalent projection for the metastable system is given in Chapter 6, Figure 6-3-3. Each region of the liquidus surface corresponds to the primary solidification of one of the five phases already present in the binary systems, namely Fe_3C , Cr_7C_3 , $Cr_{23}C_6$, ferrite α and austenite γ . In fact, the ferrite is usually designated α -Cr on the Cr-rich side and δ -Fe on the Fe-rich side, but in this temperature range, the two elements are fully miscible in the same body-centred cubic phase. The difference between the stable and metastable versions is due to the existence of an extra region in the stable diagram, corresponding to the primary solidification of graphite. The different primary solidification regions are separated by eutectic or peritectic monovariant lines.

4-5 The Fe-Cr-C system : isothermal sections and isopleths

Isotherms

In a ternary diagram, the *isotherm* T_i is a section through the diagram in the plane of the temperature T_i (*cf.* Fig. 4-5-1A). Two sorts of line can be shown on an isothermal section. They correspond to the curved boundaries of the single phase fields in the temperature plane considered and to the straight tie-lines joining the phases in equilibria. The barycentre rule is applicable to these tie-lines. For a given overall composition, it is thus possible to determine the proportions of the different phases present (*e.g.* the fractions of $M_{23}C_6$, α and liquid for a composition situated in the corresponding tie-line triangle).

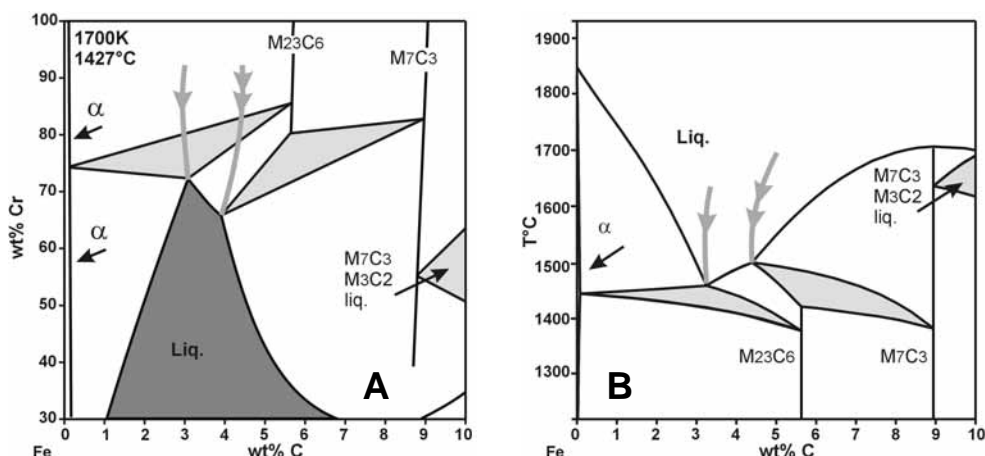


Figure 4-5-1: Fe-Cr-C system; (A) 1427 °C isotherm, (B) 80 % Cr isopleth.

The grey lines represent the eutectic and peritectic monovariant lines situated outside the plane considered. The three-phase regions concerned by these reactions (α -liquid-M₂₃C₆, liquid-M₂₃C₆-M₇C₃, liquid-M₂₃C₆-M₃C₂) are shaded light grey.

Isopleths

The isopleth C_i is a section through a ternary diagram on a plane corresponding to a fixed concentration of one of the constituents (cf. Fig. 4-5-1 B). The lines that appear represent the boundaries between the different phase fields. This representation only indicates which phases will be present for a particular composition at a given temperature. The tie-lines are not usually contained in this section, except in the particular case of a so-called *quasi-binary* section. *The lever rule cannot therefore be applied.*

The two sections shown in Figure 4-5-1 are mutually perpendicular and have a common intercept, corresponding to a chromium concentration of 80% for the isopleth and a temperature of 1427 °C for the isotherm. These unusual sections for steels were chosen because of the exemplary configuration of the phase fields. The polythermal monovariant lines shown in grey lie outside the plane of the section in each case, intersecting it at a single point. During cooling, there is a *eutectic* reaction $L \rightarrow \alpha + M_{23}C_6$, where the liquid is gradually replaced by the two solid phases. The tangent to the monovariant line cuts the α -M₂₃C₆ tie-line inside the triangle (cf. § 4-1). There is also a *peritectic* reaction $L + M_7C_3 \rightarrow M_{23}C_6$ where the liquid reacts with a solid phase already present to form a second solid phase. The tangent to the monovariant line cuts the M₂₃C₆/M₇C₃ tie-line outside the triangle.

Invariant equilibrium

At the point of intersection of two invariant lines in a ternary system, four phases are present, so that there are zero degrees of freedom and *the reaction is invariant* (Fig. 4-5-2). In this figure, three isotherms are shown for the same range of compositions,

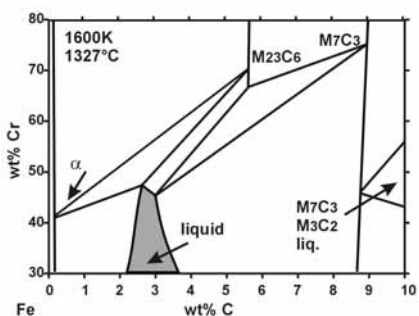
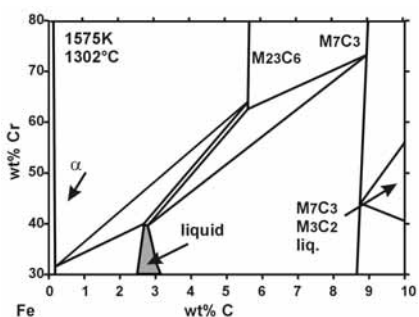


Figure 4-5-2:

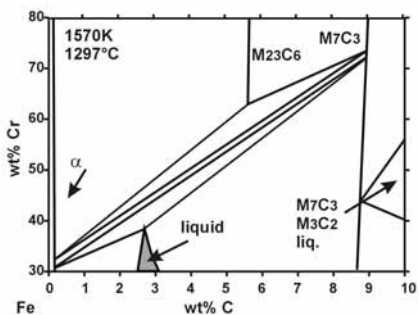
Series of 3 isothermal sections through the Fe-Cr-C diagram showing the variation of the equilibria above and below the four-phase (liquid- α -M₂₃C₆-M₇C₃) invariant equilibrium point (1299 °C). The liquid field is shaded in grey, while the α phase field is a narrow band along the Fe-Cr axis and the carbides are represented by lines, since they are considered to be perfectly stoichiometric.



At 1327 °C, there are two 3-phase equilibria :

liquid-M₂₃C₆-M₇C₃

liquid-M₂₃C₆- α



At 1302 °C, the equilibria are still the same, but the compositions of the common phases are almost, but not quite, identical.

At 1299 °C, the tie-line triangles merge to form a quadrilateral.

At 1297 °C, two new three-phase equilibria appear :

M₂₃C₆-M₇C₃- α and liquid-M₇C₃- α .

two for temperatures slightly above the invariant point at T_i and one just below it. On cooling, the two tie-line triangles merge together at T_i to form a quadrilateral, which splits again into two new triangles below T_i .

Multicomponent systems

In a system containing more than three elements, the tie-lines are no longer contained in an isothermal section, so that the barycentre rule cannot be applied geometrically. An exception is the case of a pseudo-ternary section, where the composition of one element is fixed, for example, between three stoichiometrically similar compounds A₃B/A₃C/A₃D. Isotherms and isopleths indicate only the number and nature of the phases present as a function of temperature but not their compositions.

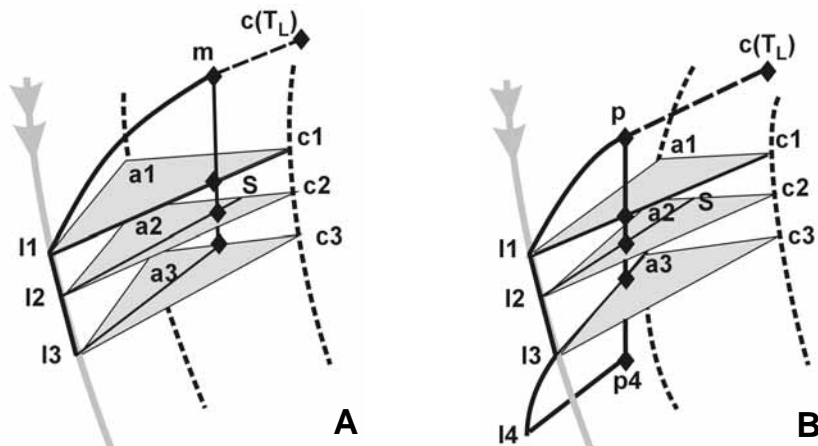


Figure 4-6-1:

Solidification paths under reversible conditions for two alloy compositions, m (diagram A) and p (diagram B), showing the variation in phase equilibria between the liquidus temperature T_L and a series of decreasing temperatures, T_1 , T_2 , T_3 and T_4 . T_3 is the solidus temperature for composition m and T_4 that for composition p . The dotted lines a_i and c_i represent the compositions of the solid phases in equilibrium with the monovariant peritectic liquid, whose composition at temperatures T_i is given by the grey lines I_i .

In A, mc_{T_L} is the first tie-line and only c phase forms down to temperature T_1 , below which a phase first begins to form. At T_2 the proportions of a_2 and c_2 in equilibrium with I_2 are respectively c_2S/a_2c_2 and a_2S/a_2c_2 . At T_3 , m lies on the tie-line a_3c_3 and the liquid is completely consumed.

In B, the solidification stages at T_1 and T_2 are the same as in A, but the liquid is not exhausted at T_3 , so that below this temperature it is in equilibrium only with the a phase. The liquid is exhausted at T_4 .

4-6 The Fe-Cr-C system : solidification paths

Reversible conditions

When a liquid alloy is cooled under so-called reversible conditions, it is assumed to go through a series of equilibrium states between the liquid and the homogeneous solid phases. The principle of conservation of mass dictates that *all the tie-lines* must pass through the composition of the initial liquid (*i.e.* that of the alloy as a whole).

The solidification path is the locus of the liquid composition as the temperature falls. The two solidification paths analysed in Figure 4-6-1 A and B have been chosen for two different alloy compositions, respectively m and p , with two solid phases designated a and c . By comparison with the two previous figures, the solid phases could be $M_{23}C_6$ and M_7C_3 .

In diagram A, the liquidus surface is reached at temperature T_L where the only solid to form is c , with composition c_{TL} , mc_{TL} being the first tie-line. The liquidus composition then moves down to meet the monovariant peritectic line l at temperature T_1 , below which the second solid phase a begins to form by reaction between the liquid and c . Since there is not yet any a phase, the alloy composition m lies on the tie-line between l_1 and c_1 . At the lower temperature T_2 , the line l_2m cuts the tie-line a_2c_2 at point S, the lever rule defining the relative proportions of the two solid phases (and also of liquid and solid along l_2mS). At the temperature T_3 , the alloy composition m lies on the tie-line a_3c_3 and the liquid is completely exhausted.

In diagram B, for alloy composition p , the major difference is that at temperature T_3 , p lies on the tie-line l_3a_3 , so that the c phase has now been completely consumed before the liquid is fully exhausted. During further solidification down to the solidus temperature T_4 , only the a phase continues to form.

Solidification without diffusion in the solid phase

Permanent equilibrium between the liquid and solid can rarely be maintained during practical solidification conditions, due to the slow rates of diffusion in the solid phases. It is therefore useful to consider another extreme situation, where the liquid remains effectively fully homogeneous, but is in equilibrium with the solid only at the interface, *no diffusion* occurring within the solid phase. This situation corresponds to what are known in solidification theory as the Scheil-Gulliver conditions (§ 5-1 and 5-2). The solidification path is still defined by the locus of the liquid compositions during cooling. *As under reversible conditions, it begins at the liquidus point in the direction defined by the corresponding liquid-solid tie-line in the plane of compositions.* The liquid is enriched or depleted in solute elements due to the formation of solid in which their concentrations are lower or higher respectively. On further cooling, the process is repeated, with the new liquid composition as the starting point at each temperature (Fig. 4-6-2). The solidification path comes to an end when the liquid is exhausted, at a temperature still termed the solidus.

In Figure 4-6-2, the two types of solidification path are illustrated for an alloy composition situated in the primary M_7C_3 carbide liquidus surface. In the absence of diffusion in the solid, the phases formed are successively, primary M_7C , peritectic $M_{23}C_6$, eutectic $M_{23}C_6$ and α , eutectic M_7C_3 and α , then (not illustrated) eutectic M_7C_3 and γ and eutectic M_3C and γ . The last liquid to solidify has the composition of the eutectic with the lowest melting point.

To avoid confusion, the end of the solidification path is denoted T_{Sth} for the case of full equilibrium and total homogeneity in the solid phases and T_{Sp} for the case of only partial or no diffusion. It should be noted that, under non-equilibrium conditions, the solidification path always crosses peritectic lines, as illustrated in this example.

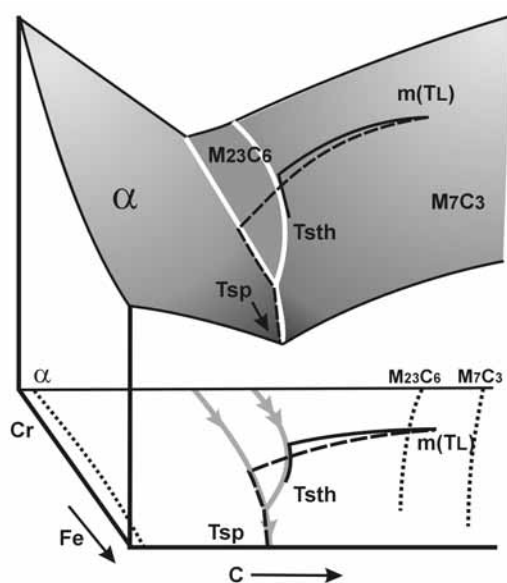
In practice, some diffusion occurs in the solid, and solidification paths closer to real conditions are analysed in § 6-3.

Figure 4-6-2:

Examples of solidification paths in the Fe-Cr-C system, in both reversible conditions (full lines) and without diffusion in the solid (dashed lines). Perspective view and projection in the composition plane.

The grey arrowed lines are the projections of the peritectic and eutectic monovariant lines in the composition plane, while the dotted lines are the projections of the α , $M_{23}C_6$ and M_7C_3 compositions associated with the monovariant equilibria.

The path $m_{TL}-T_{Sth}$ corresponding to reversible equilibrium conditions stops at the point where the liquid is exhausted. The path $m_{TL}-T_{Sp}$ corresponding to the absence of diffusion in the solid crosses the peritectic line, then follows the eutectic line down to what in this case is the binary invariant eutectic point γ/M_3C (not shown), where solidification is completed at constant temperature.



In a binary diagram, the solidification path follows the liquidus line, whereas in a ternary it follows the liquidus surface. An exception to this rule is the case of a quasi-binary section, i.e. a section through a ternary system represented as a binary, for example Fe-WC, Fe-VC or Fe-NbC. The XC carbides have a precise stoichiometric ratio between carbon and the element X, so that the liquidus-XC tie-lines all lie in the Fe-XCT plane. A “binary” reasoning of this sort is valid only when the tie-lines are coplanar. However, the eutectic Fe/XC is not invariant (since the amounts of C and X dissolved in the iron in equilibrium with XC can vary).

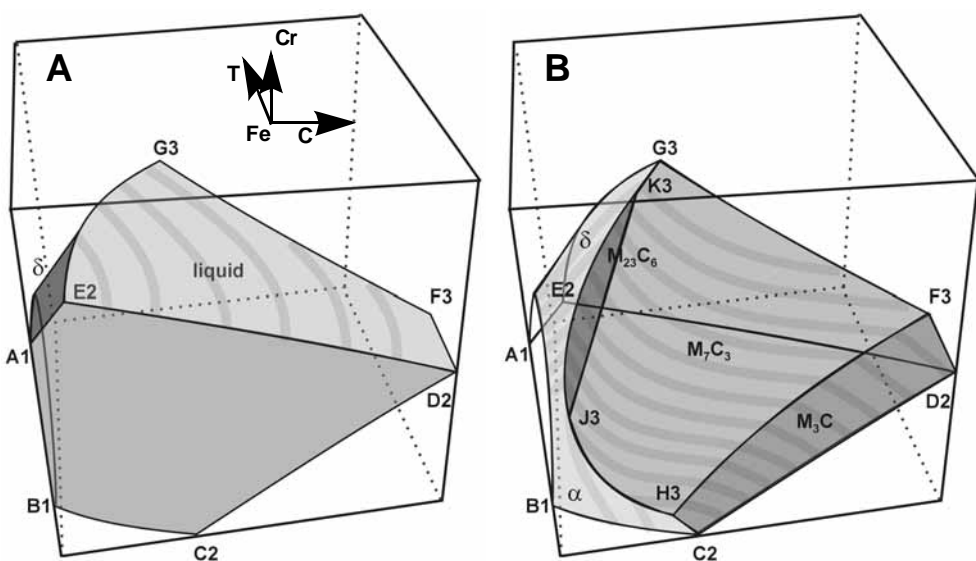
The term “pseudo-binary” will be reserved for the representation of a section between two compounds in a system of n elements, without implications concerning the positions of the tie-lines. An example is the $Fe_3C-V_4C_3$ system [Rag84]. The principles applicable to binary systems (lever rule, solidification paths) are not valid in this case.

4-7 The Fe-Cr-C system : the austenite field

Perspective views, isothermal sections and isopleths

A precise knowledge of the limits of the austenite field and of the associated equilibria is of vital importance for steels based on this system.

- In particular, for compositions lying outside the austenite field at all temperatures, it is impossible to obtain a martensitic structure by quenching.

*Figure 4-7-1:*

Perspective view of the austenite phase field in the metastable Fe-Cr-C system.

A) Phase field boundaries corresponding to the γ /liquid (*solidus*) and γ / δ -ferrite (*solvus*) equilibria. The phases in equilibrium with the austenite are indicated on the corresponding boundary surfaces.

B) Solvus surfaces bounding the austenite field. The invariant points are labelled with a figure representing the number of phases in equilibrium with austenite. The characteristics of the invariant equilibria are given in the table below.

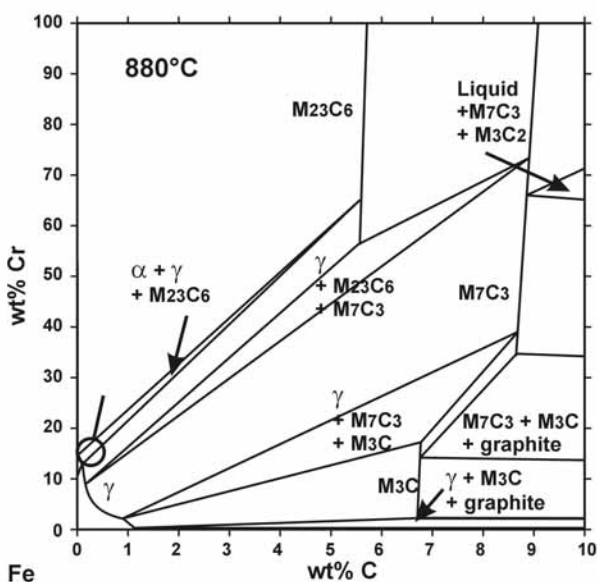
Invariant reactions	Austenite composition C and Cr wt.%	Temperature °C	Phases in equilibrium with austenite
A1	0C-0Cr	1394	δ -ferrite
B1	0C-0Cr	912	α -ferrite
C2	0.76C-0Cr	727	α -ferrite/ M_3C
D2	2.14C-0Cr	1147	liquid/ M_3C
E2	0.16C-0Cr	1493	δ -ferrite/liquid
F3	2C-4.35Cr	1178	liquid/ M_7C_3/M_3C
G3	0.77C-19.8Cr	1284	liquid/ M_7C_3/δ -ferrite
H3	0.59C-1.28Cr	749	α -ferrite/ M_7C_3/M_3C
J3	0.10C-7.9Cr	814	α -ferrite/ $M_{23}C_6/M_7C_3$
K3	0.61C-18.8Cr	1209	δ -ferrite/ $M_{23}C_6/M_7C_3$

- Furthermore, the type of carbides in equilibrium can have a marked influence on properties, especially the corrosion resistance.

Figure 4-7-1 shows two perspective views illustrating the three-dimensional shape of the austenite phase field and its relationship with the adjacent phases with which it is in

Figure 4-7-2:

Calculated 880 °C section of the Fe-Cr-C system. The phases present are indicated only for the single and three-phase fields. The “magnifying glass” indicates the $\alpha/\gamma/M_{23}C_6$ field, also shown in the 14% Cr isopleth below.



equilibrium, together with the associated invariant lines and points. the connection between the different maps, lines and invariants points in equilibrium with austenite.

The fields of existence of the various carbides at 880 °C can be seen in the isothermal section shown in Figure 4-7-2. The carbon axis has been extended to 10 wt.% to completely include the three-phase triangles. The carbides M_3C , M_7C_3 and $M_{23}C_6$ are represented by straight lines, corresponding to precise stoichiometry, and although the diagram is calculated on this assumption, it is very nearly the case in reality. The proportion of $M_{23}C_6$ carbide at 880 °C can be evaluated by applying the barycentre rule to the tie-line triangle $\alpha/\gamma/M_{23}C_6$. The amount is very small in the composition range corresponding to 14 % Cr steels. The 14 % Cr isopleth is shown in Figure 4-7-3 and is limited to 1 % C to focus essentially on the austenite field.

The addition of chromium markedly changes the extent of the austenite field, which disappears completely at about 20 % Cr. This is illustrated in Figure 4-7-4 in which a series of isopleths from 0 to 19 % Cr are superimposed. This simplified diagram was first published in 1962 [Rob62] and has since been reproduced in many textbooks on the metallurgy of stainless steels. The version shown in Figure 4-7-4 is an updated form, based on isopleths calculated using the recently optimised Fe-Cr-C diagram. It indicates the transition between the M_7C_3/γ and $M_{23}C_6/\gamma$ fields, materialised by the position of the three-phase field. From a practical standpoint, it should be noticed that, the higher the chromium content, the more the range of stability of M_7C_3 is pushed to higher temperatures. Constant carbon isopleths are also frequently employed, since they reveal the modifications induced by carbon in the Fe-Cr system. Figure 4-7-5 shows a calculated isopleth for 0.1 % C and is little different to the experimental version published in 1958 [Bun58].

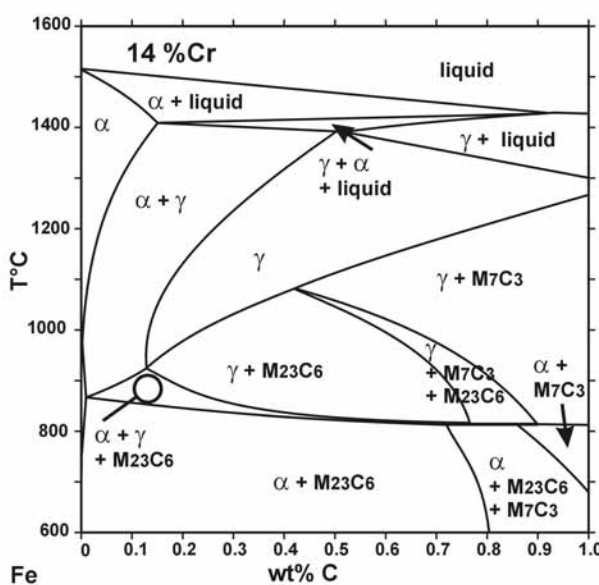


Figure 4-7-3:
Calculated 14 % Cr isopleth for the Fe-Cr-C system. This diagram indicates the phases present under equilibrium conditions. The “magnifying glass” indicates the $\alpha/\gamma/M_{23}C_6$ field, also shown in the 800 °C isotherm above.

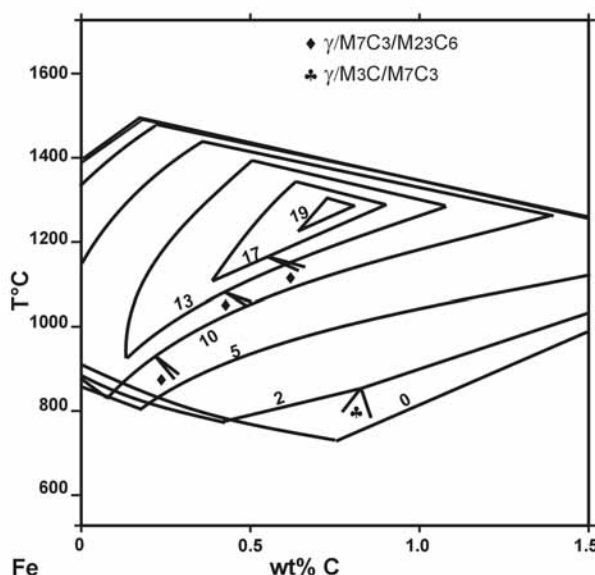


Figure 4-7-4:
Calculated isopleths for different Cr contents in the Fe-Cr-C system. Only the limits of the austenite field are shown, together with indications of the junction with the $\gamma/M_3C/M_7C_3$ and $\gamma/M_7C_3/M_{23}C_6$ three-phase fields.

Figure 4-7-5:

Calculated 0.1% C isopleth for the Fe-Cr-C system.

